

Dark matter halo’s and self similarity

Alard, C.

Institut d’Astrophysique de Paris, 98bis boulevard Arago, 75014 Paris, France

email:alard@iap.fr

ABSTRACT

This paper explores the self similar solutions of the Vlasov-Poisson system and their relation to the gravitational collapse of dynamically cold systems. Analytic solutions are derived for power law potential in one dimension, and extensions of these solutions in three dimensions are proposed. Next the self similarity of the collapse of cold dynamical systems is investigated numerically. The fold system in phase space is consistent with analytic self similar solutions, the solutions present all the proper self-similar scaling. An additional point is the appearance of an $x^{-\frac{1}{2}}$ law at the center of the system for initial conditions with power law index larger than $-\frac{1}{2}$ (the Binney conjecture). It is found that the first appearance of the $x^{-\frac{1}{2}}$ law corresponds to the formation of a singularity very close to the center. Finally the general properties of self similar multi dimensional solutions near equilibrium are investigated. Smooth and continuous self similar solutions have power law behavior at equilibrium. However cold initial conditions result in discontinuous phase space solutions, and the smoothed phase space density loses its auto similar properties. This problem is easily solved by observing that the probability distribution of the phase space density P is identical except for scaling parameters to the probability distribution of the smoothed phase space density P_S . As a consequence P_S inherit the self similar properties of P . This particular property is at the origin of the universal power law observed in numerical simulation for $\frac{\rho}{\sigma^3}$. The self similar properties of P_S implies that other quantities should have also an universal power law behavior with predictable exponents. This hypothesis is tested using a numerical model of the phase space density of cold dark matter halo’s, an excellent agreement is obtained.

Key words: cosmology: dark matter

1 INTRODUCTION.

The Vlasov-Poisson system for a space space density $f(\mathbf{x}, \mathbf{v}, t)$ potential $\phi(\mathbf{x})$ and density $\rho(\mathbf{x})$, is:

$$\frac{\partial f}{\partial t} + \frac{\partial f}{\partial \mathbf{x}} v - \frac{\partial f}{\partial \mathbf{v}} \frac{\partial \phi}{\partial \mathbf{x}} = 0 \quad (1)$$

$$\Delta \phi = q_n G \rho \quad (2)$$

$$\rho = \int f d^n v \quad (3)$$

2 SCALE FREE SOLUTIONS.

The scale free solutions should be consistent with the following condition:

$$f(\lambda_1 \mathbf{x}, \lambda_2 \mathbf{v}, \lambda_3 t) = \lambda_4 f(\mathbf{x}, \mathbf{v}, t) \quad (4)$$

Considering the special case, $\lambda_i = 1 + \epsilon d\lambda_i$, and expanding to the first order in ϵ , we obtain the following equation:

$$\frac{\partial f}{\partial \mathbf{x}} d\lambda_1 \mathbf{x} + \frac{\partial f}{\partial \mathbf{v}} d\lambda_2 \mathbf{v} + \frac{\partial f}{\partial t} d\lambda_3 t - f d\lambda_4 = 0 \quad (5)$$

the solution to Eq. (5) reads:

$$f(\mathbf{x}, \mathbf{v}, t) = f_0 t^{\alpha_0} F\left(\frac{\mathbf{x}}{t^{\alpha_1}}, \frac{\mathbf{v}}{t^{\alpha_2}}\right) \quad (6)$$

With:

$$\alpha_0 = \frac{d\lambda_4}{d\lambda_3}, \quad \alpha_1 = \frac{d\lambda_1}{d\lambda_3}, \quad \alpha_2 = \frac{d\lambda_2}{d\lambda_3}$$

3 SCALE FREE SOLUTION OF THE VLASOV EQUATION.

Inserting Eq. (6) in Eq. (1) will test the possibility that scale invariant solutions of the Vlasov equation do exist. We define the following scaled variables: $\mathbf{x}_2 = \frac{\mathbf{x}}{t^{\alpha_1}}$, $\mathbf{v}_2 = \frac{\mathbf{v}}{t^{\alpha_2}}$. Using the former notations, a solution of the type given in Eq. (6) is a solution of the Vlasov equation if:

$$(2 + n\alpha_2)F + (1 + \alpha_2) \frac{\partial F}{\partial \mathbf{x}_2} \mathbf{x}_2 + \alpha_2 \frac{\partial F}{\partial \mathbf{v}_2} \mathbf{v}_2 - \left(\frac{\partial F}{\partial \mathbf{x}_2} \mathbf{v}_2 + \frac{\partial \tilde{\phi}}{\partial \mathbf{x}_2} \frac{\partial F}{\partial \mathbf{v}_2} \right) = 0 \quad (7)$$

And:

$$\alpha_0 = -2 - n\alpha_2, \quad \alpha_1 = 1 + \alpha_2 \quad (8)$$

We define: $\tilde{\phi}(\mathbf{x}_2) = t^{-2\alpha_2} \phi(\mathbf{x})$.

Note that an equation similar to Eq. 8 was already derived by Lancellotti and Kiessling (2001).

4 ONE DIMENSIONAL SOLUTIONS.

We will study the solution in the 2 dimensional phase space (x,v) , which corresponds to $n=1$ in Eq (7) for a power law potential.

$$\tilde{\phi}(x_2) = k|x_2|^{\beta+2} \quad (9)$$

The variable is re-scaled x_2 so that $k = \frac{1}{2}$. The following change of variable $u = |x_2|^\eta$, is introduced with $\eta = \frac{\beta}{2} + 1$ in Eq (7). It is assumed that $-2 < \beta < 0$, as a consequence the exponents of $\tilde{\phi}$ and u are positive. The corresponding equation for the variable u is:

$$2 + \alpha_2 + (1 + \alpha_2)\eta \frac{\partial G}{\partial u} u + \alpha_2 \frac{\partial G}{\partial v_2} v_2 - \text{sgn}(x_2)\eta \left(\frac{\partial G}{\partial u} v_2 - 2ku \frac{\partial G}{\partial v_2} \right) u^{\frac{\beta}{\beta+2}} = 0 \quad (10)$$

Where $\text{sgn}(x)$ is the function:

$$\text{sgn}(x) = \begin{cases} -1 & x < 0 \\ 1 & x \geq 0 \end{cases}$$

And $\log(F(x_2, v_2)) = G(u, v_2)$ We now introduce again new variables, (R, ψ) , with:

$$\begin{aligned} R &= \sqrt{u^2 + v_2^2} \\ \cos \psi &= \begin{cases} \frac{u}{R} & x_2 \geq 0 \\ -\frac{u}{R} & x_2 < 0 \end{cases} \end{aligned}$$

The new equation in these variables is:

$$2 + \alpha_2 - \eta_2 \cos \psi \sin \psi (1 + \alpha_2) \frac{\partial H}{\partial \psi} + R (\cos^2 \psi (1 + \alpha_2) \eta_2 + \alpha_2) \frac{\partial H}{\partial R} + \eta \frac{\partial H}{\partial \psi} (R |\cos(\psi)|)^{\frac{\beta}{\beta+2}} = 0 \quad (11)$$

Where $\eta_2 = \eta - \frac{\alpha_2}{1+\alpha_2}$, and $H(R, \psi) = G(u, v)$.

An interesting case is when the potential $\phi(x)$ is stationary, which corresponds to, $\beta\alpha_1 = -2$ and to $\eta_2 = 0$. In this case Eq. (11) is reduced to:

$$2 + \alpha_2 + R\alpha_2 \frac{\partial H}{\partial R} + \frac{\alpha_2}{1 + \alpha_2} \frac{\partial H}{\partial \psi} (R |\cos(\psi)|)^{-\frac{1}{\alpha_2}} = 0 \quad (12)$$

Eq. (12) has a general solution:

$$H(R, \psi) = -\frac{\alpha_2 + 2}{\alpha_2} \log R + Q \left(R^{-\frac{1}{\alpha_2}} + \frac{1 + \alpha_2}{\alpha_2} \int |\cos(\psi)|^{\frac{1}{\alpha_2}} d\psi \right) \quad (13)$$

Eq (11) has an asymptotic solution for small R (and all values of η_2), the term in $R^{\frac{\beta}{\beta+2}}$ that multiply the ψ derivative of H dominates other derivatives of H . The solution is:

$$H(R, \psi) = -\frac{(\alpha_2 + 2)}{\frac{\beta}{2} + 1} R^{-\frac{\beta}{\beta+2}} \int |\cos \psi|^{-\frac{\beta}{\beta+2}} d\psi + H_2(R) \quad (14)$$

For a stationary potential, which corresponds to $\beta\alpha_1 = -2$, Eq. 14 is reduced to:

$$H(R, \psi) = -\frac{(\alpha_2 + 1)(\alpha_2 + 2)}{\alpha_2} R^{\frac{1}{\alpha_2}} \int |\cos \psi|^{\frac{1}{\alpha_2}} d\psi + H_2(R) \quad (15)$$

Note that developing the general solution in Eq. (13) for $\eta_2 = 0$, small R , and adopting $Q = -(2 + \alpha_2) \ln + Q_2$ we obtain:

$$H(R, \psi) \simeq \frac{1 + \alpha_2}{\alpha_2} \int |\cos \psi|^{\frac{1}{\alpha_2}} d\psi \left(-(\alpha_2 + 2)R^{\frac{1}{\alpha_2}} + Q_2'(R^{-\frac{1}{\alpha_2}}) \right) + Q_2(R^{-\frac{1}{\alpha_2}})$$

Provided that $Q_2'(R^{-\frac{1}{\alpha_2}})$ is of lower order than $R^{\frac{1}{\alpha_2}}$ the former expression reduces to Eq. (15). Note that if Q_2 behaves at origin like a power law with negative exponent this condition will be satisfied, and that as consequence the behavior of the Q_2 solution at origin will not be singular, which is a condition for the validity of the approximation at small R . As a consequence the general solution and the approximation at small R are consistent for $\eta_2 = 0$.

5 GEOMETRY OF THE SOLUTION.

To study the geometry of the solution the iso-contours of the solutions will be investigated. Considering a contour with phase space density F_0 , and using Eq. 13, the equation of the corresponding contour is:

$$\bar{Q} \left(R^{-\frac{1}{\alpha_2}} + I(\psi) \right) = R^{\frac{\alpha_2+2}{\alpha_2}} F_0 \quad (16)$$

With the following definitions:

$$Q = \ln \bar{Q} \quad \text{and} \quad I(\psi) = (1 + \alpha_2) \int |\cos(\psi)|^{\frac{1}{\alpha_2}} d\psi \quad (17)$$

It is easy to realize that Eq. 16 corresponds to the equation of a spiral in phase space. Since $I(\psi) \simeq k\psi$ where k is a constant, the equation reduces to $R = s(\psi)$, a specific example is a logarithmic spiral which would occur if s is a power law plus a constant. An important parameter of this spiral structure is the inter-fold distance. This parameter is straightforward to measure in numerical simulations, and can be easily compared to the analytic expectation. The variation of ψ between 2 consecutive folds is 2π , thus if the position on one fold is ψ_0 the corresponding position on the consecutive is $\psi_1 = \psi_0 + 2\pi$. We will assume that the folds corresponds to a large number of turns, consequently $\psi_0 \gg 2\pi$, and $I(\psi_1) = I(\psi_0) + \int_0^{2\pi} |\cos(\psi)|^{\frac{1}{\alpha_2}} d\psi = I_0 + \epsilon I_1$, with $\epsilon \ll 1$. Similarly we write the inter fold variation of $R_1 = R_0 + \epsilon dR$. Inserting these expression in Eq. 16, and using the original

equation we obtain:

$$\frac{dR}{R_0} = \frac{P(R_0^{\frac{\alpha_2+2}{\alpha_2}} F_0) I_1 \alpha_2}{P(R_0^{\frac{\alpha_2+2}{\alpha_2}} F_0) R_0^{-\frac{1}{\alpha_2}} + \alpha_2 + 2} \quad (18)$$

With:

$$P(u) = \frac{\bar{Q}'(\bar{Q}^{-1}(u))}{u} \quad (19)$$

Requiring that all functions are power law's and starting with Q , then Eq. 19 implies that P is also a power law. If $\frac{dR}{R}$ is also a power law Eq. 18 implies $P(u) \propto u^{\frac{1}{\alpha_2}}$, and as a consequence we have:

$$\frac{dR}{R_0} = \frac{F_0^{\frac{1}{\alpha_2+1}} I_1 \alpha_2}{F_0^{\frac{1}{\alpha_2+2}} + \alpha_2 + 2} R_0^{\frac{1}{\alpha_2}} \propto R_0^{\frac{1}{\alpha_2}} \quad (20)$$

An interesting consequence of Eq. 20 is the prediction of the projected density caustics. Introducing $R = x^{\frac{\beta}{2}+1}$ and $\alpha_2 = -\frac{2}{\beta} - 1$, the position p_n is n^{th} fold is:

$$p_n = n^{\frac{2}{\beta}} \quad (21)$$

The self similar solution of Bertschinger (1985) corresponds to $\beta = -\frac{9}{4}$ which implies $p_n = n^{-\frac{8}{9}}$. Sikivie & Kinney (2001) proposed the following numerical approximation, $p_n \simeq \frac{1}{n}$ which is quite close to the prediction of Eq. 21. It is important to note that the thickness of a given contour can be derived using the same method as the inter-folds distance. The variation of position for a contour in Eq. 16 corresponds to a variation of $I(\psi_1) = I(\psi_0 + d\psi)$, where $d\psi$ corresponds to a differential in the initial conditions for two opposite sides of the contour. As a consequence the calculations are identical to the calculations performed for the inter-fold distance, and the contour thickness is proportional to the inter-fold distance.

6 MULTI DIMENSIONAL SOLUTIONS.

It is useful to define the coordinates in the 6D space, $(\mathbf{x}_2, \mathbf{v}_2)$, and the corresponding modulus of distances r and velocities v . The solution in several dimensions is constructed using the results obtained in one dimension, the solution is the sum of a general solution plus a special solution. To facilitate the calculations we introduce $G(\mathbf{x}_2, \mathbf{v}_2) = \log F(\mathbf{x}_2, \mathbf{v}_2)$, and a power law potential $\tilde{\phi}(r) = \frac{1}{2}r^{\beta+2}$, $-2 < \beta < 0$, Eq. 7 then reads:

$$\begin{aligned} (2 + n\alpha_2) + P_1 + P_2 &= 0 \\ P_1 &= (1 + \alpha_2) \frac{\partial G}{\partial \mathbf{x}_2} \mathbf{x}_2 + \alpha_2 \frac{\partial G}{\partial \mathbf{v}_2} \mathbf{v}_2 \\ P_2 &= -\frac{\partial G}{\partial \mathbf{x}_2} \mathbf{v}_2 + (\beta + 2) r^{\beta+1} \mathbf{x}_2 \frac{\partial G}{\partial \mathbf{v}_2} \end{aligned} \quad (22)$$

If we consider a solution of the type:

$$G(\mathbf{x}_2, \mathbf{v}_2) = K_0(R) + K_1(r, v_r) \quad (23)$$

Here $R = \sqrt{v^2 + r^{\beta+2}}$, and $K_1(r, v_r)$ is a function of the distance modulus and radial velocity v_r . The special solution K_1 is constructed using the method we developed for the one dimensional solution. Provided we substitute the $(|x|, v)$ space with the (r, v_r) space the equations are the same, and finding the solution K_1 is thus a problem we have already solved. Assuming that K_1 is a full solution or an asymptotic solution for small R , we introduce the solution Eq. (23) in Eq. (22). Thus considering $G = K_0 + K_1$ the only remaining significant terms may come from K_0 only. Since basically K_0 is a function of energy, we have $P_2 = 0$. Using the R variable, we find that P_1 behaves like $R \frac{\partial K_0}{\partial R}$. Since the terms relative to K_1 are of order of unity, the P_1 term of K_0 must be compared to unity. Provided that the function K_0 behaves like a power law with positive exponent, the relevant P_1 term will become negligible at small R and the solution in Eq. (23) is an asymptotic solution at small R .

7 ONE DIMENSIONAL COLD COLLAPSE.

7.1 Power law regime in the central region.

The evolution of a system of particles with small initial velocity dispersion in the two dimensional phase space under the action of one dimensional planar gravity will be investigated in this section. Interestingly Binney, (2004) found that for such systems the density near the center of the system is very close to $x^{-\frac{1}{2}}$. This power law density suggests the possibility of a universal self-similar regime in the central region. Binney, (2004) propose that the $x^{-\frac{1}{2}}$ regime is valid for a very large class of initial conditions, but an interesting problem is to find for what type of initial conditions the $x^{-\frac{1}{2}}$ is not obtained, and where is the limit. This problem may be solved using the following simple approach, we take a set of cold initial conditions with power law densities and compute the density of the system at late times. The initial power law is constructed using a random generator. The trajectories of the particles are estimated by a direct computation of the 1D force (without any smoothing), and an update of the velocity and position using a simple leapfrog method. The results of the 1D numerical simulations ($4 \cdot 10^5$ points) are presented in Fig. 1. For a better numerical efficiency the power law exponent of the force β_F is computed, the force is much smoother than the density (affected by caustics), the equivalent projected density exponent, is $\beta_F - 1$.

Interestingly the initial exponent β is conserved at later time for $\beta < -\frac{1}{2}$, while for larger values of β the final exponent has a constant value of $-\frac{1}{2}$ (see Fig. 1). As a consequence the $x^{-\frac{1}{2}}$ density at the center is not universal but does occur precisely when $\beta = -\frac{1}{2}$. Note that this effect was also noticed by Schulz et al (2012) with results quite similar to Fig. 1. This particular behavior suggests a cut-off, no final exponent is larger than $-\frac{1}{2}$. To understand the cause of this cut-off it is interesting to investigate numerical simulation with initial conditions $\beta > -\frac{1}{2}$ and look for the first appearance of the $x^{-\frac{1}{2}}$ power law. This analysis is illustrated for $\beta = -\frac{1}{3}$, the first appearance of the $x^{-\frac{1}{2}}$ projected density occurs when the the first fold starts to form or equivalently just after the first crossing of particles with opposite velocities at the center. The phase space structure at this time is presented in Fig. 2, we notice that near the center we have two caustics. These two caustics are very close to the center and according to the theory of singularities for a one dimensional density, we expect that their projected density will go like $\tilde{x}^{-\frac{1}{2}}$, where \tilde{x} is a coordinate centered on the caustic. This is just what we obtain in Fig. 3, the lower fold (red points in Fig. 2) has a projected density close to $\tilde{x}^{-\frac{1}{2}}$ near the center. This density starting from the caustics extends at distances significantly larger than the separation between the caustic and the center, which means that in a large portion of this regime $\tilde{x} \simeq x$ and that as a consequence the density goes like $x^{-\frac{1}{2}}$. The $\tilde{x}^{-\frac{1}{2}}$ regime assume that the phase space density along the fold is constant, but due to the high non-linearity at the crossing the stretching of the phase space is large which implies that the density along the fold is nearly constant in a significant domain. This density associated with the caustic initiate the $x^{-\frac{1}{2}}$ asymptotic regime at the center and since it is dominant for $\beta > -\frac{1}{2}$ it is prone to extend to larger values of x . At later times the systems forms a large number of folds, with the persistence of the initial caustic induced $x^{-\frac{1}{2}}$ regime at the center. The $x^{-\frac{1}{2}}$ central regime is also present for other initial conditions, for instance, a Gaussian, 2 Gaussian,..., and many other, but the difference is that this even if this regime is present very close to the center we find also a rather brutal transition to a tiny area with nearly constant density. This transition occurs at the very center of the system, and the size of this constant region depends on the initial conditions. This constant region at the center is probably a remain of the nearly flat density present in some initial conditions. The transition from the $x^{-\frac{1}{2}}$ regime to the constant density regime signal also a break of the self similar regime. In any case the presence of this small constant region affect the extent of the $x^{-\frac{1}{2}}$ regime which is still present and most likely for reasons similar

to the power law initial conditions. For a further investigation of this issue it is interesting to point the contribution of S. Colombi (2012) on this particular topic.

7.2 Self similarity in the central region.

It is important to note that in the central region of all numerical simulations self-similarity was observed (see Fig. 7 for an illustration). The exponent $-\frac{1}{2}$ of the density implies $\alpha_2 = 3$, which means that in the x dimension the simulation should scale like $\frac{1}{t^3}$ and in the v dimension like $\frac{1}{t^4}$. Using these scaling the folds at different times should be at the same location, which could be verified with good accuracy. This property definitely proves that the $x^{-\frac{1}{2}}$ corresponds to a self similar regime in phase space. Since analytic formula for the self-similar solution with power law density were derived in the former sections, it is interesting to check the consistency with the fold system. The fold system is illustrated in Fig.'s 4 and 5. For power law initial conditions, it is expected that all quantities will be power laws, and thus the inter-fold distance should be given by Eq. 20. The potential $\phi(x)$ was computed, as well as $R = \sqrt{v^2 + \phi}$, and finally the inter-fold distance dR was estimated. The results are presented in Fig. 6. The exponent of the inter-fold distance as a function of R according to Eq. 20 is $\gamma = \frac{1}{\alpha_2} + 1$ and provided that α_2 is deduced from the initial condition exponent β_0 , we have, $\alpha_2 = -\frac{2}{\beta_0} - 1$ and $\gamma = \frac{2}{\beta_0 + 2}$. Fig. 6 shows that this theoretical expectation of γ is in good agreement with the numerical estimations. It is interesting to note that we expect that the theoretical expectation of γ is going to match the data for $\beta_0 < -\frac{1}{2}$, but for $\beta_0 > -\frac{1}{2}$ we would expect $\beta = -\frac{1}{2}$ and not $\beta = \beta_0$, this is not what is observed, and we must conclude that despite the $x^{-\frac{1}{2}}$ law at the center the structure of the fold system is preserved for $\beta_0 < -\frac{1}{2}$. Other type of initial conditions imply different inter-fold distance, but this is always a small correction from the $dR \propto R^\gamma$ law. To conclude it is interesting to note that all solutions for a large class of initial conditions have all a power law density with exponent $-\frac{1}{2}$ at the center, and are all self-similar with the same similarity index at the center. This definitely indicates that the degree of freedom (Q in Eq. 13 or H_2 in Eq. 14) is important since it allows some flexibility to accommodate the initial conditions. All solutions have similar density at the center but have different phase distributions while at the same time they remain self-similar.

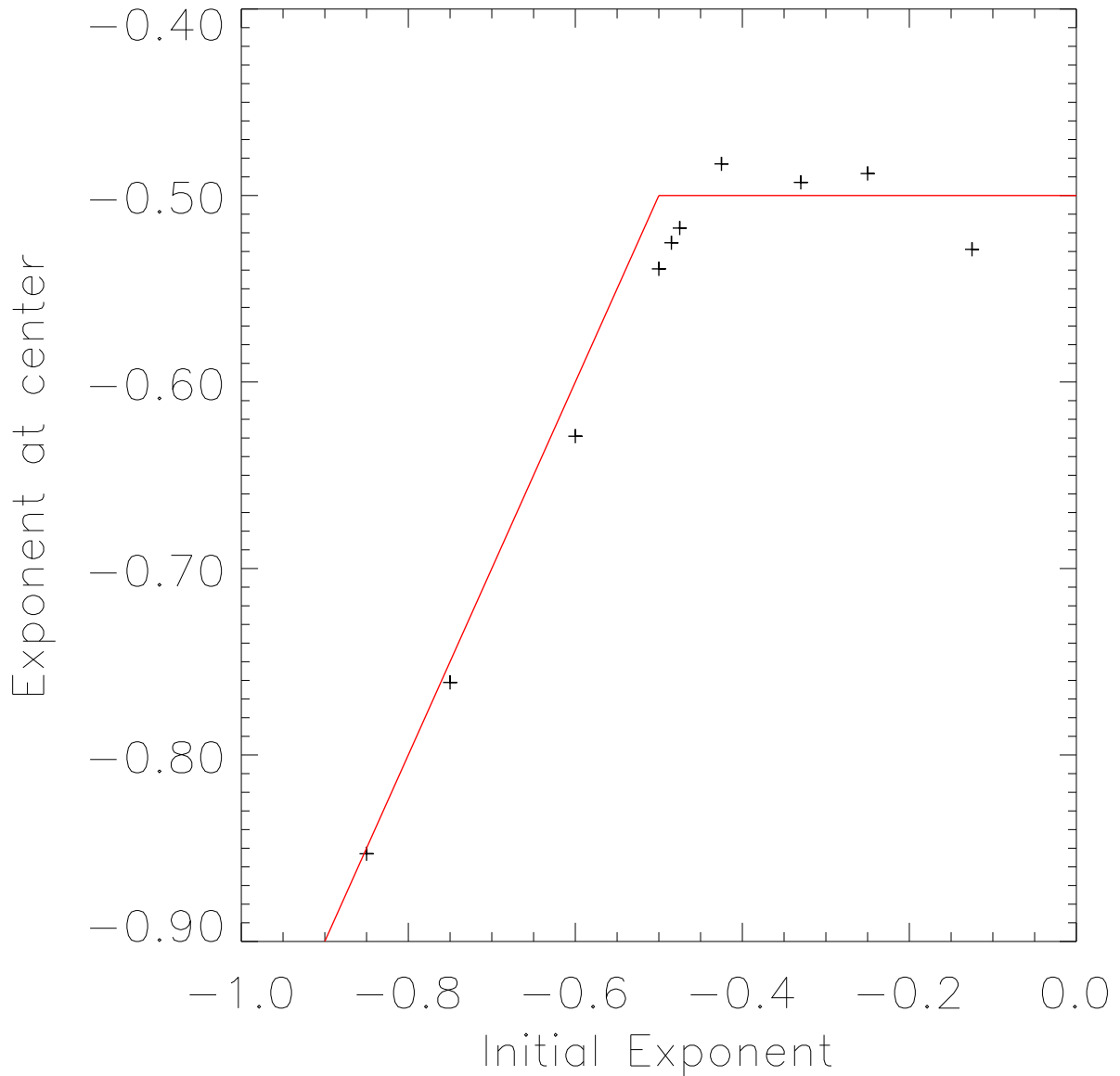


Figure 1. The power law exponent of the late time projected density as a function of the initial power law exponent. Note that the exponent was evaluated by fitting a power law to the force, and making the necessary conversion.

8 PROPERTIES OF STATIONARY SELF-SIMILAR SOLUTIONS IN MULTI DIMENSIONS.

The collapse of a dark matter halo in cosmological conditions is a very different problem from the 1D collapse investigated in the former section. Here self similarity is imposed by the cosmological infall, the self similarity is not a consequence of a singularity at the center or of power law initial conditions. In cosmology the initial stage of the halo formation can be represented with the accretion of matter on a seed mass. This process implies that the turn-

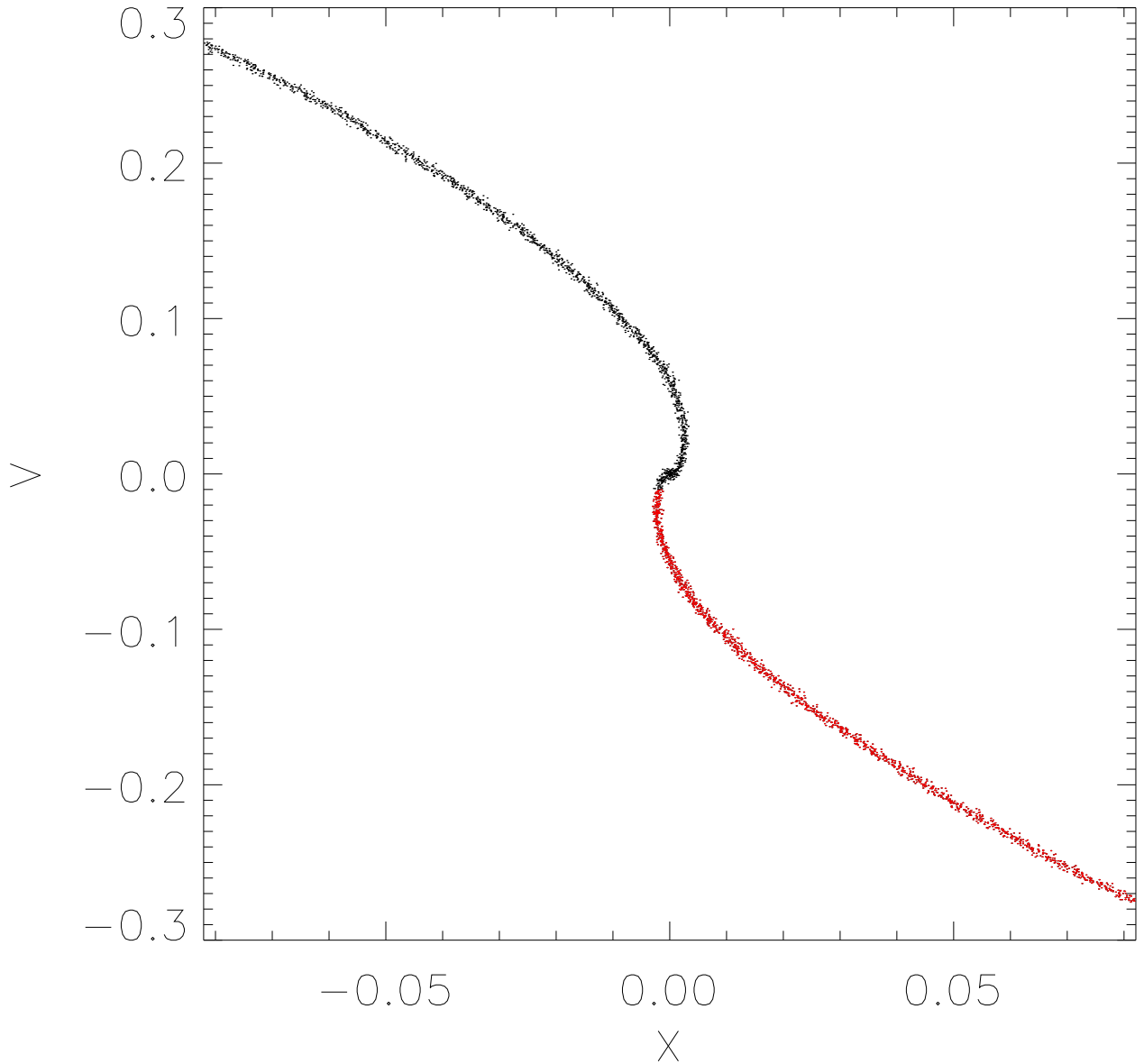


Figure 2. The phase space structure corresponding to cold initial near the first crossings of particles for an initial cold velocity distribution with density profile $x^{-\frac{1}{3}}$.

over radius of the in-falling shells of matter is a power law of time (Gunn 1977, Bertschinger, 1985). The relevant similarity exponent in the notations of this paper is $\alpha_2 = -\frac{1}{9}$. The self similarity of the solution is enforced by the cosmological infall, which implies that the final solution should reflect the similarity of the infall (Taylor & Navarro 2001). Thus we have good reasons to assume that the final outcome of the collapse of a dark matter halo will corresponds to a self-similar solution of the Vlasov-Poisson system. Since dark matter is cold the solution will correspond to the multiple folds of the initial surface in phase space.

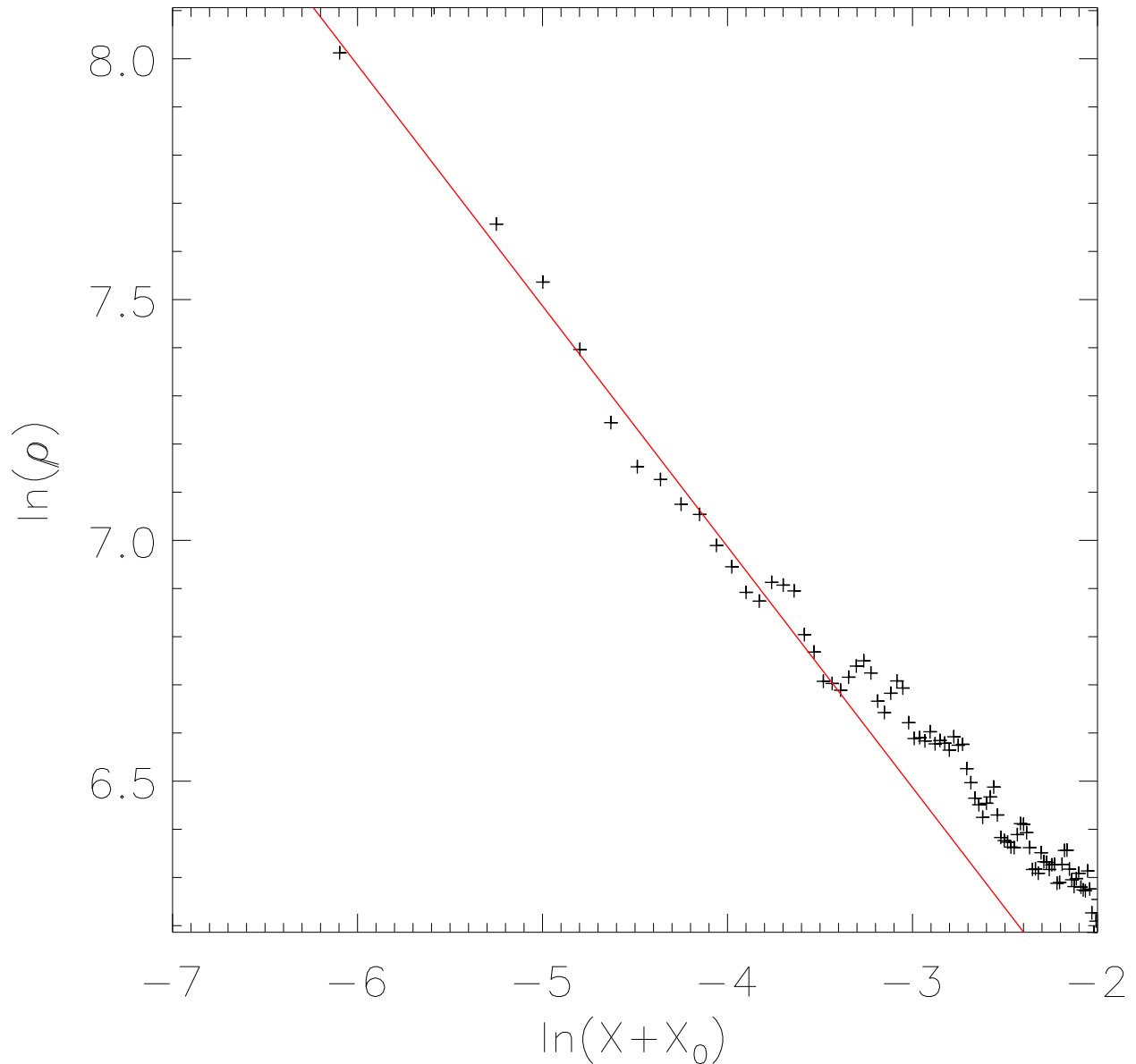


Figure 3. The projected density associated with the first caustic (red points in Fig. 3). To demonstrate the relation between the power law projected density and the caustic, the x coordinate system was re-centered on the caustic position. The red-line represents a power law with exponent $-\frac{1}{2}$.

However, an equilibrium or a near equilibrium situation is a very different problem for a smooth continuous system in phase-space and for the folding of a cold system in phase space. Cold systems form spirals in phase space and even in their late evolution they will be still evolving and will neither converge to a smooth continuous equilibrium system. The smoothing of the spiral will produce a smooth phase-space density, and that smoothed density will be nearly stationary at late times. However in general the problem is that the smoothed density is not necessarily auto-similar. The smoothed density will correspond to

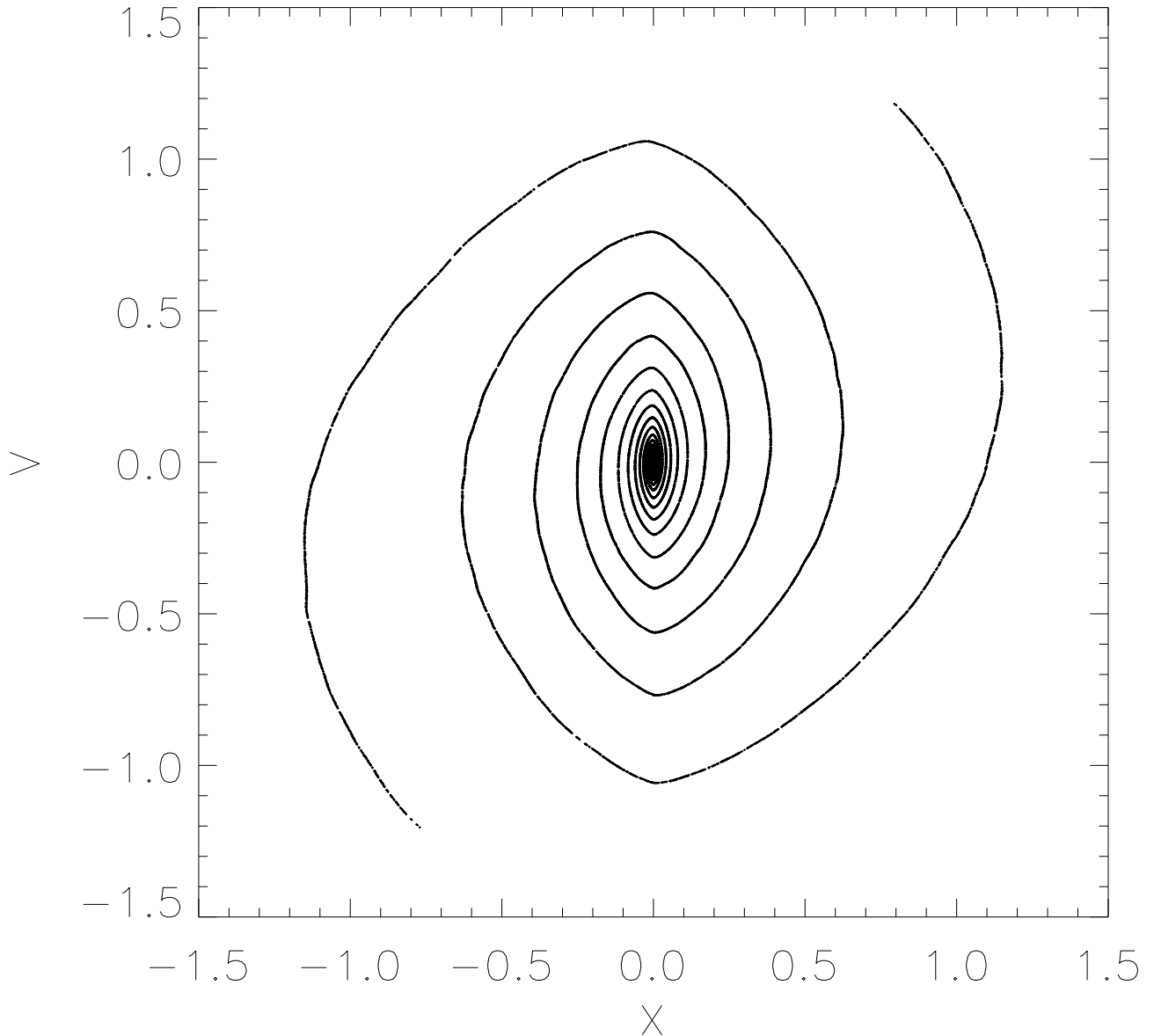


Figure 4. The evolution of the cold system with initial density profile $x^{-\frac{1}{3}}$ at later times.

the smooth auto-similar solution only in some special cases. This problem is due to the fact that the smoothed phase space density does not satisfy the ordinary Vlasov equation but a different differential equation. Since we cannot relate the cold self-similar solutions to the smooth self-similar solutions we cannot benefit from the fact that the smooth equilibrium solutions are simple analytic functions (Lancellotti & Kiessling, 2000). However it is clear that at late time the cold self similar solution should have a nearly stationary smoothed density in phase space and that it will corresponds to a given sub-set of self similar solution. The final problem is thus to identify the properties of this sub-set of solutions. A key point

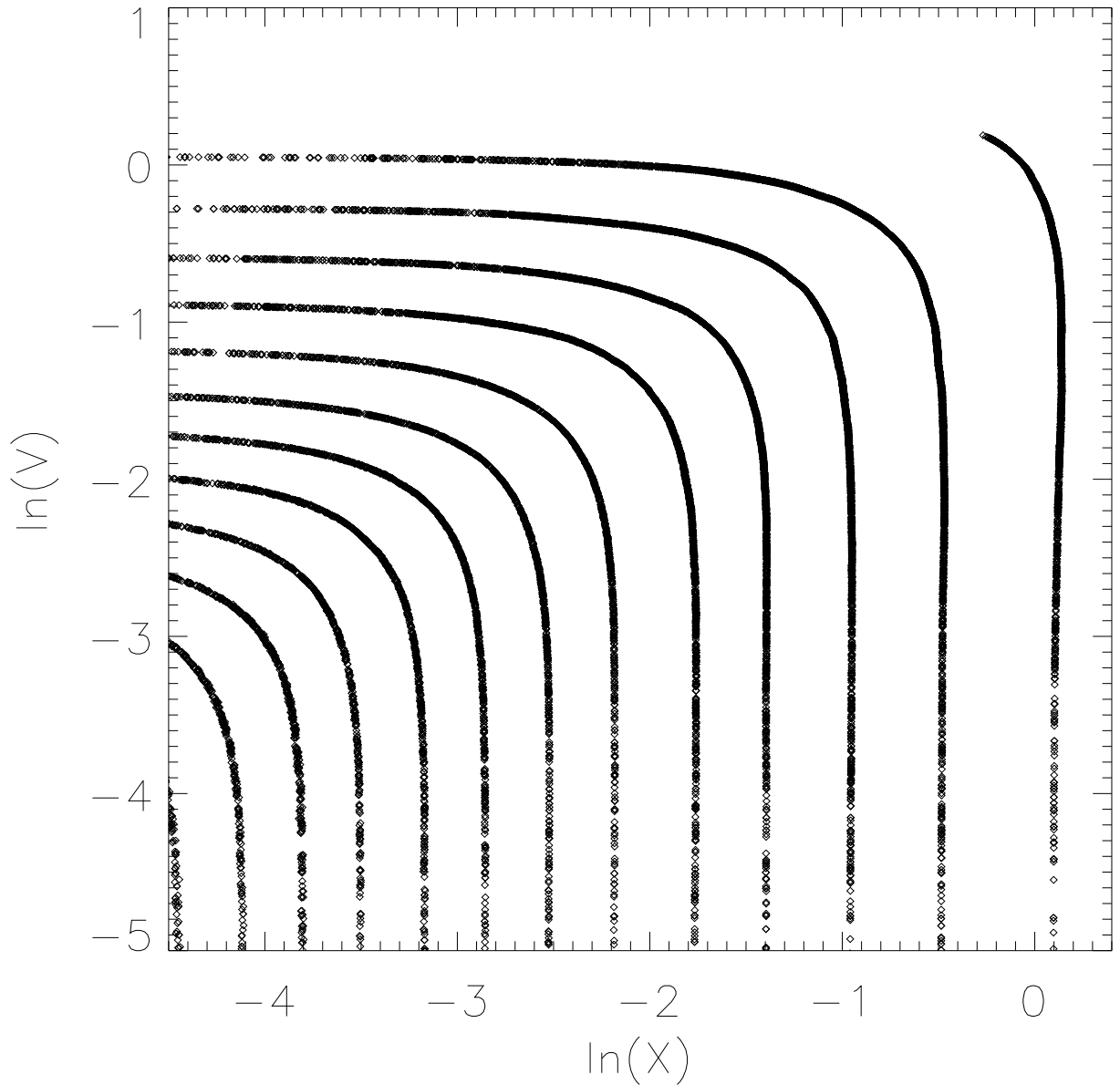


Figure 5. Upper part ($x > 0, v > 0$) of the phase space diagram presented in Fig. 4. Logarithmic coordinates were used for both axis for a better view of the space folds.

in the solution of this issue is to observe that even if the cold solution is discontinuous in phase space, the probability distribution of the phase space density, $P(f)$ could be similar to that of a smooth solution $P_S(f)$. Actually if we consider the local surfaces of folds in phase space within some small solid angle, the integrated density between two local surfaces would corresponds to the local surface multiplied by the thickness of the fold. The integration and averaging of the density between two folds corresponds to the smoothing operation. If the fold thickness is proportional to the distance between the folds, then the smoothed

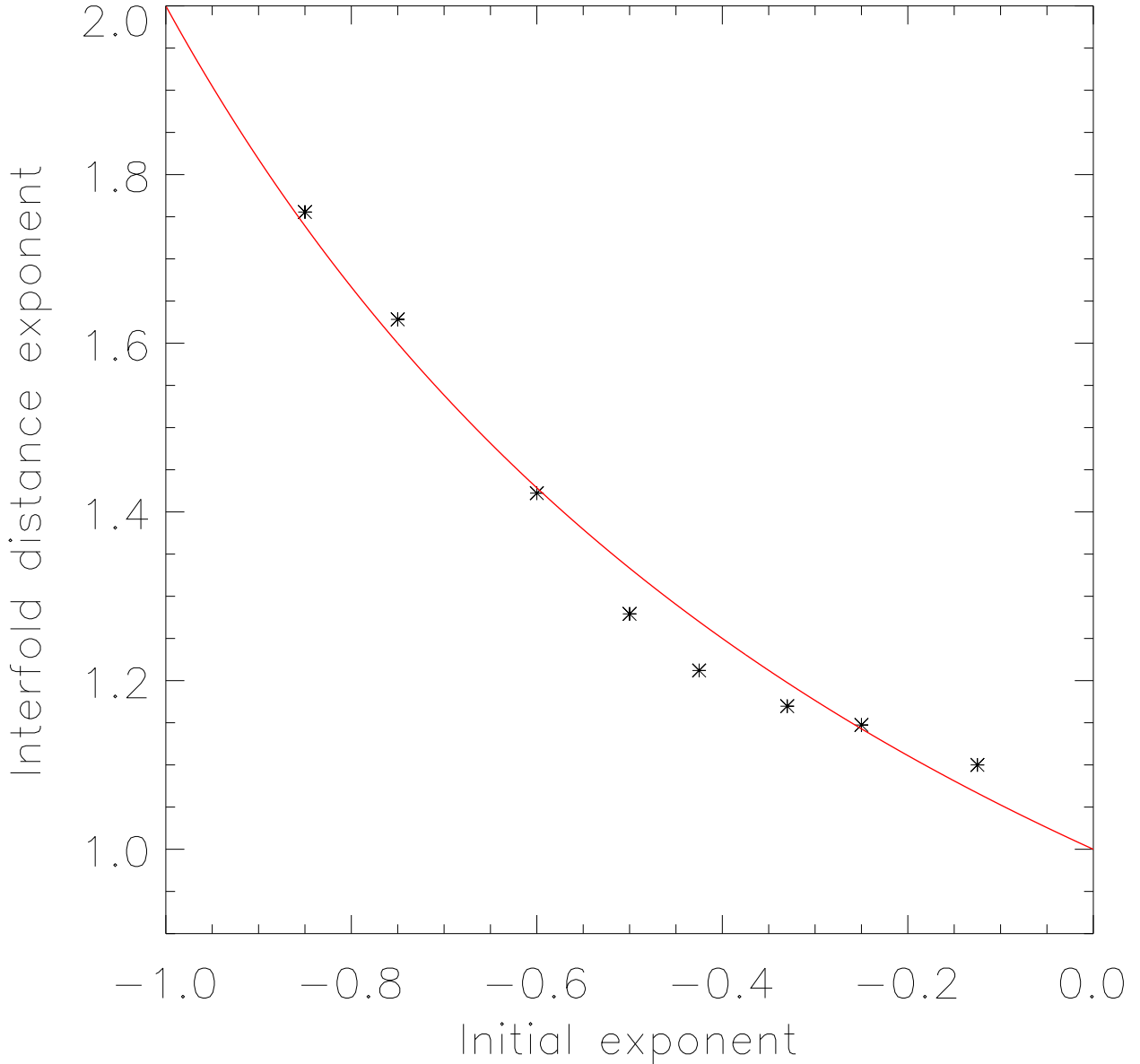


Figure 6. The power law exponent of the inter-fold distance reconstructed using the numerical simulation data. The continuous line corresponds to the theoretical expectation (see Eq. 20).

density will be proportional to the cold un-smoothed density, and its occurrence will also be proportional to the cold occurrence since it is proportional to the ratio between the thickness and the inter-fold distance. This reasoning shows that the smoothed probability density of f can be deduced from the un-smoothed density by the introduction of constant scale factors (see Fig. 8 for an illustration). As a consequence the self-similar properties of the cold probability distribution will be also valid for the smooth probability distribution. Note that f is made of many different contours, but since the scaling properties between P and P_S

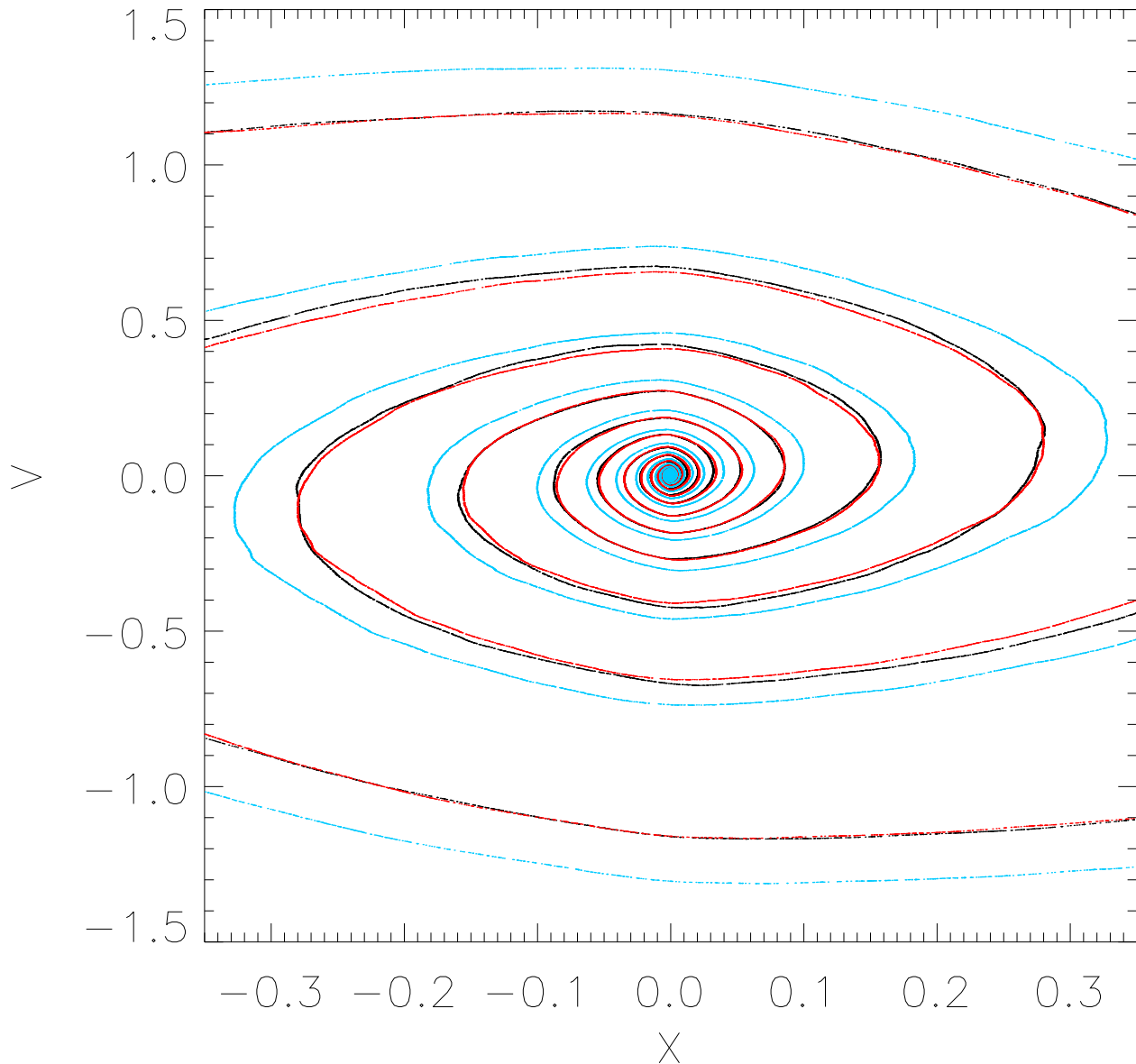


Figure 7. The fold system at the center at two different times (black and blue) for the power-law simulation with $\beta = -\frac{1}{3}$. The blue folds are re-scaled using $\alpha_2 = 3$, with a time-scaling equal to the ratio of the time from the beginning of the simulation for each fold system.

are valid for each contour, the transfer of self similarity between P and P_S remain valid in presence of many different contours. The property of proportionality between the thickness and the inter fold distance was demonstrated in Sec. 5, but is also required for the existence of the solution. If the thickness exceeds the inter fold distance then a crossing would occur near the origin, while if the opposite behavior happened the crossing would happen on larger distances. The only solution is thus that the fold thickness is proportional to the fold inter distance. As a consequence it is clear that the smooth probability distribution inherit the self

similar properties of the cold solution, and that power-law integrated quantities estimated from $P_S(f)$ should have an auto-similar behavior. Note that a priori the equivalence between $P(f)$ and $P_S(f)$ is valid on any sub domain of the phase space, provided that this domain is large enough to define the statistics of f . In particular all quantities like:

$$Q_n(\mathbf{x}_0) = \int P_S(f(\mathbf{x}, \mathbf{v})) f(\mathbf{x}, \mathbf{v})^n d\mathbf{f} \quad \text{With : } \mathbf{x} = \mathbf{x}_0 \quad \text{and : } -\infty < \mathbf{v} < \infty$$

have to be self similar since

$$Q_n^0(\mathbf{x}_0) = \int P(f(\mathbf{x}, \mathbf{v})) f(\mathbf{x}, \mathbf{v})^n d\mathbf{f} \quad \text{With : } \mathbf{x} = \mathbf{x}_0 \quad \text{and : } -\infty < \mathbf{v} < \infty$$

Is self-similar and P_S inherit the self similarity of P . As a consequence the Q_n function should write as a power law of time multiplied with a function of \mathbf{x}_2 . A direct estimate of the mean value of f Q_1 is:

$$Q_1(\mathbf{x}) = \int P_S(f) f df \simeq \frac{1}{8n^3\sigma^3} \int_{-n\sigma}^{n\sigma} f d^3v \propto \frac{\rho}{\sigma^3}$$

In the same spirit one may approximate Q_n :

$$Q_n(\mathbf{x}) \propto \frac{\int f^n dv}{\sigma^3}$$

The ratio of Q_n quantities is also self-similar:

$$R_{nm} = \frac{Q_n}{Q_m}$$

Since Q_n and R_{nm} are smooth continuous functions and self similar:

$$Q_n(\mathbf{x}) = t^{n\alpha_0} h_1(\mathbf{x}_2)$$

and

$$R_{nm}(\mathbf{x}) = t^{(n-m)\alpha_0} h_2(\mathbf{x}_2)$$

Stationary solutions for Q_n and R_{nm} implies that h_1 and h_2 are power law's, thus:

$$Q_n(r) \propto t^{n\alpha_0} \left[\frac{r}{t^{\alpha_1}} \right]^{\gamma_1} = r^{\gamma_1} \quad ; \quad \gamma_1 = n \frac{\alpha_0}{\alpha_1} = -n \frac{15}{8}$$

Similarly:

$$R_{nm}(r) \propto t^{(n-m)\alpha_0} \left[\frac{r}{t^{\alpha_1}} \right]^{\gamma_2} = r^{\gamma_2} \quad ; \quad \gamma_2 = -(n-m) \frac{15}{8}$$

(Note that we assume isotropic systems, thus \mathbf{x} was replaced with the distance modulus r .)

The calculation of integrals involving higher order power of f (f^n , $n > 1$) requires the knowledge of the spatial distribution of f . The reconstruction of f from numerical discrete numerical data is a difficult and uneasy task (See Arad, Dekel, & Klypin, 2004). A more convenient way of estimating the higher order terms is to use the accurate analytic approximations of f that were developed by Wojtak, *etal.* (2008). All integrals were performed using Eq. 29 from Wojtak, *etal.* (2008). The results are presented in Fig.'s 9 and

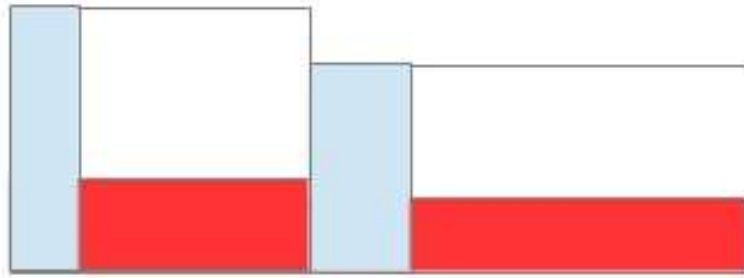


Figure 8. The cold un-smoothed density is represented in blue and the local value of the smoothed density is represented in red in this simple 1D analogy. The cold density is at the position of the fold and its thickness is proportional to the inter-fold distance. The smooth density corresponds to the averaging of the cold density between two consecutive folds. Since the thickness and the inter-fold distance are proportional, the construction of the smooth density is equivalent to a simple re-scaling of the cold density. Obviously the cold and smoothed density cannot be proportional in all points of phase space, since the cold density is zero in some place, and the smooth density is neither equal to zero between folds. However the distribution of the values of the smooth and cold density differs only by scale factors, which implies that the self similar (scaling) properties of the cold distribution of f values are preserved in the smooth density distribution, or probability distribution of the smooth f .

10. For convenience an inverse power law's of higher order quantities were taken to reduce all self similar exponents to the $-\frac{15}{8}$ theoretical self-similar expectation. All quantities are nearly linear in the log-log diagram, and all slopes in this diagram are very close to $-\frac{15}{8}$. The only possible explanation is that if all moments of the smooth probability distribution $P_S(f)$ are self similar is that $P_S(f)$ itself is self similar. As a consequence the universal behavior observed for CDM halo's in numerical simulations reflects the self similarity of $P_S(f)$.

The author would like to thank Scott Tremaine for support during his stay at the Institute for advanced studies in 2011.

REFERENCES

- Arad, I., Dekel, A., Klypin, A., 2004, MNRAS, 353, 15
 ertschinger Bertschinger, E., 1985, ApJS, 58, 39
 Binney J., 2004, MNRAS, 350, 939
 Colombi, S., 2012, in preparation
 Gunn, J.E., 1997, ApJ, 218, 592
 Lancellotti, C., Kiessling, M., 2001, ApJ, 549, L93
 ancillotti Schulz, A., Dehnen, W., Jungman, G., Tremaine, S., arXiv:1206.0299v1
 Sikivie, P., Kinney, W., 2001, Annals of the New York Academy of Sciences, vol. 927, issue 1, pp. 102-109
 Taylor, J.,E., Navarro, J., F., 2001, ApJ, 563, 483
 Wojtak, R., Lokas, E. L., Mamon, G. A., Gottlober, S., Klypin, A., Hoffman, Y., 2008, MNRAS, 388, 815

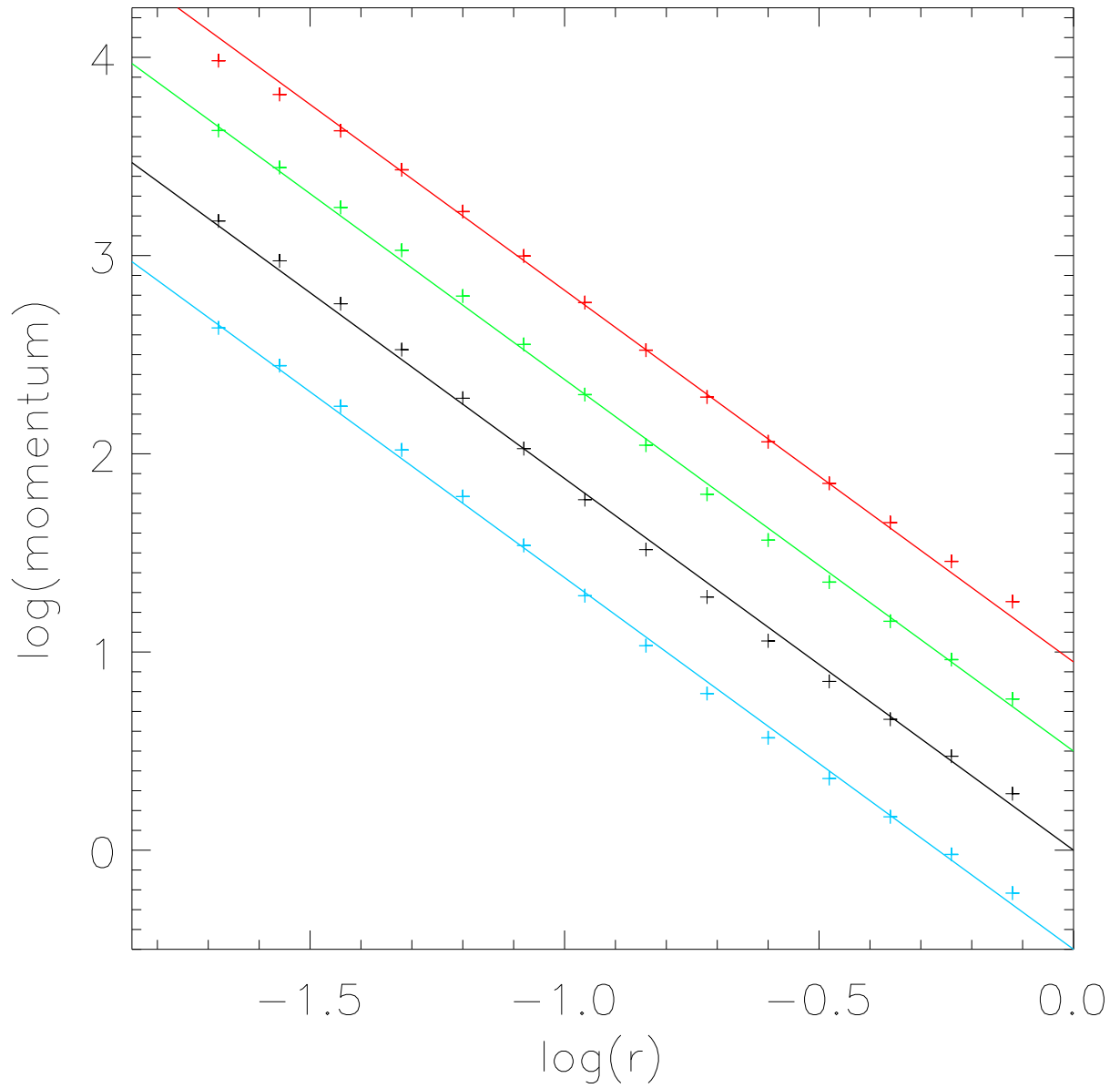


Figure 9. The following quantities $\frac{\rho}{\sigma^3}$ black, $\left[\frac{f f^2 d^3 v}{\sigma^3}\right]^{\frac{1}{2}}$ blue, $\left[\frac{f f^3 d^3 v}{\sigma^3}\right]^{\frac{1}{3}}$ green, $\left[\frac{f f^4 d^3 v}{\sigma^3}\right]^{\frac{1}{4}}$ red, are represented by points (cross). The points were calculated using the Wojtak et al. (2008) model. A straight line with slope $-\frac{15}{8}$ is over-plotted over each curve.

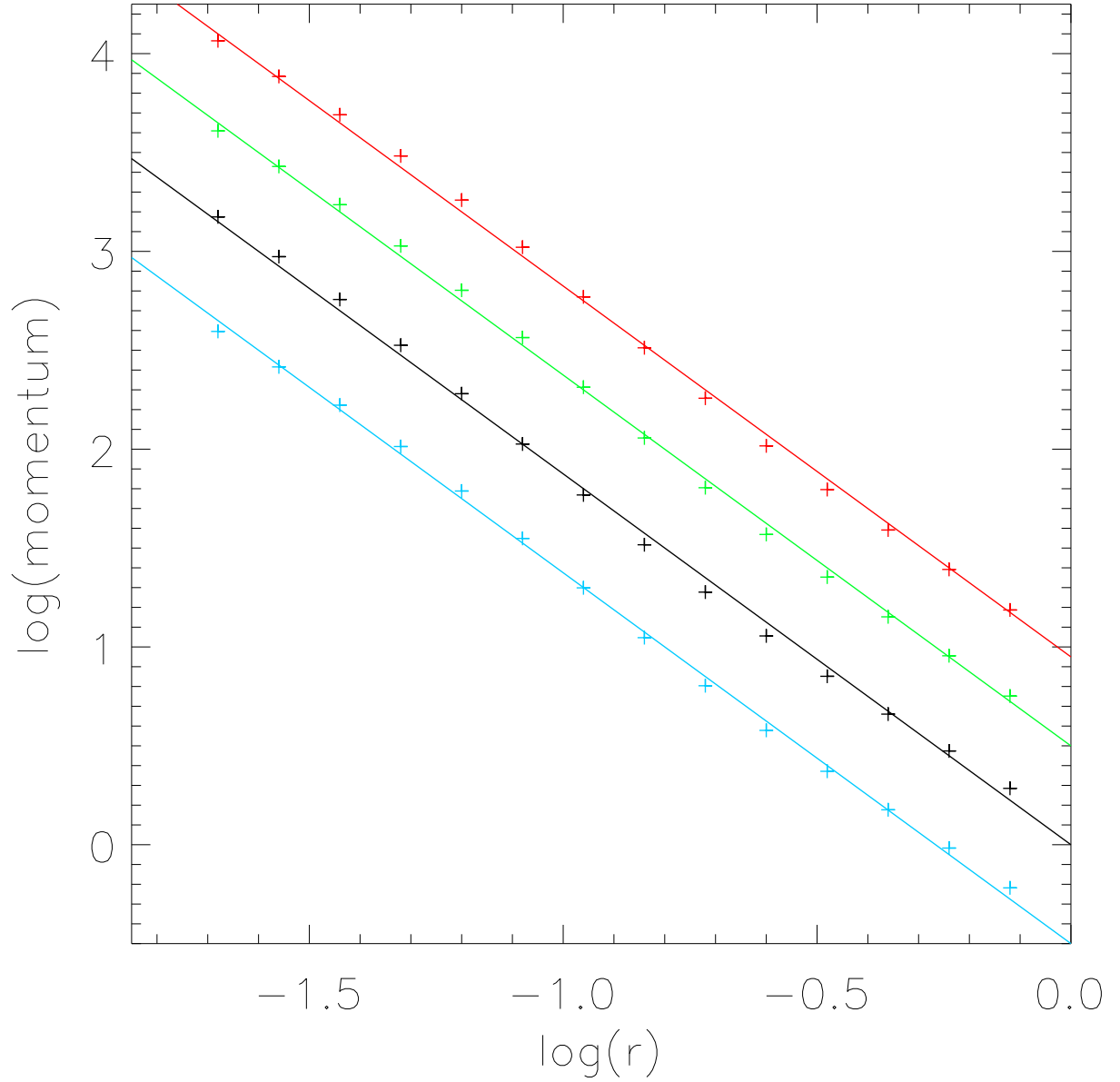


Figure 10. The following quantities $\frac{\rho}{\sigma^3}$ black, $\frac{\int f^2 d^3 v}{\int f d^3 v}$ blue, $\left[\frac{\int f^3 d^3 v}{\int f d^3 v}\right]^{\frac{1}{2}}$ green, $\left[\frac{\int f^4 d^3 v}{\int f d^3 v}\right]^{\frac{1}{3}}$ red, are represented by points (crosses). The points were calculated using the Wojtak et al. (2008) model. A straight line with slope $-\frac{15}{8}$ is over-plotted over each curve.

